

RESEARCH ARTICLE | FEBRUARY 28 2024

Surface plasmon resonance (SPR) sensor for measurement of glucose and ethanol concentrations

Lia Aprilia ; Dedi Riana; Wildan Panji Tresna; Imam Tazi; Ratno Nuryadi



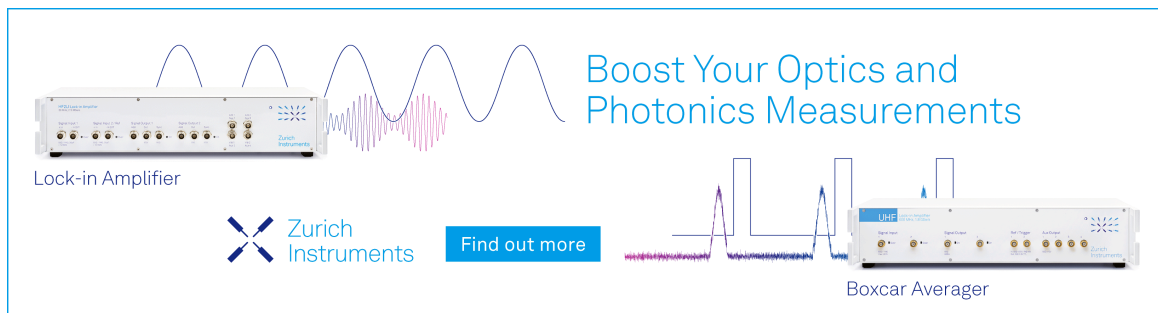
AIP Conf. Proc. 3003, 020106 (2024)

<https://doi.org/10.1063/5.0186536>




CrossMark

Boost Your Optics and Photonics Measurements



Lock-in Amplifier



Find out more

Boxcar Averager

Surface Plasmon Resonance (SPR) Sensor for Measurement of Glucose and Ethanol Concentrations

Lia Aprilia^{1, a)}, Dedi Riana^{2, b)}, Wildan Panji Tresna^{1, c)}, Imam Tazi^{2, d)},
and Ratno Nuryadi^{1, e)}

¹Research Center for Photonics, Research Organization for Nanotechnology and Materials, National Research and Innovation Agency, South Tangerang, Banten 15314, Indonesia

²Department of Physics, Universitas Islam Negeri Maulana Malik Ibrahim Malang, Malang, East Java 65144, Indonesia

^{a)} Corresponding author: liao003@brin.go.id

^{b)} ddediriana@gmail.com

^{c)} wild004@brin.go.id

^{d)} tazimam1974@gmail.com

^{e)} ratno.nuryadi@brin.go.id

Abstract. Surface Plasmon Resonance (SPR) has been extensively applied as a sensor because of its high sensitivity, accurate selectivity, label-free and real-time biomolecular interactions. In this work, simulation and experiment have been studied on the concentration measurement of ethanol and glucose solutions by SPR sensors. The sensor design used a Kretschmann configuration consisting of Glass/Cr/Au and was simulated by using Finite Difference Time Domain (FDTD) method. The ethanol and glucose solutions with varied concentrations were injected into the SPR channel, and the resonance angle was monitored. For the glucose concentration measurement, the resonance angle increases (from 71.607° to 74.434°) as the glucose concentration increases (from 0% to 15%) with a sensitivity of about 111.71°/RIU. These experimental results agree with the simulation result, which showed a good linear response for the glucose concentration. However, for the ethanol measurement, an increase in resonance angle to the ethanol concentration is not linear in the higher concentration, which is related to the change in the refractive index. However, the excellent correlation between the experiment and simulation results shows that the SPR sensor has good sensitivity and accuracy.

INTRODUCTION

Nowadays, the optical phenomena of metals are still being studied. One of the phenomena arising from the coating of thin metal films on a dielectric substrate is a plasmonic effect, which is the consequence of the interaction between light and the free electrons of the metal film. The results of theoretical and experimental studies related to the fundamentals of plasmonics are provided by many works of scientists [1-4]. The basic phenomenon in plasmonics is the presence of surface waves called Surface Plasmon Polaritons (SPPs). These surface waves appear at the dielectric-metal interface when one illuminates the interface by incident light [1]. The SPPs consist of collective oscillation of surface electron density of the metal part on the dielectric-metal interface [3]. The applications of plasmonics are very wide such as for chemistry [5], biomedical sensing [6], food control [7], environment [8], etc. It is known that SPR sensors are one of the applications of plasmonics, here, we report our work regarding SPR sensors.

SPR sensors employ the SPR phenomena as the signal response of the sensor. The principle of the SPR sensor is easy to understand. When the metal-dielectric interface is illuminated by p-polarized light, the metal part's free electron oscillates and excites SPPs, which are electromagnetic (EM) waves. Therefore, the SPPs have a propagation constant. If the propagation constant of the incident light $\beta_{\text{incident light}}$ is equal to the propagation constant of SPPs β_{SPPs} , the resonance will occur. The physical parameter of the resonance can be observed by observing the reflected light

intensity that the minimum will show it reflected light intensity [9]. SPR sensors can be used in various applications, such as temperature sensors [10], biosensors [11], chemical sensors [12, 13], etc., with a configuration of grating-based, prism-based SPR, and waveguide/fiber optic-based SPR [14].

It is interesting to study SPR in aqueous conditions, such as the detection of glucose or alcohol, which can potentially be developed in wide applications. Many researchers reported measurement systems of glucose and ethanol concentrations using an interferometer, spectroscopic refractometry, or polarimeter methods [15-17]. However, the configurations of these methods are not simple. Using SPR, it is possible to get simple measurements, compact size, real-time, and fast response. In this work, glucose and ethanol concentrations were investigated by simulation (FDTD method) and experiment. We analyzed the shift of the resonance angle of SPR due to the various concentration of ethanol and glucose. The results from the simulation and experiment were discussed.

EXPERIMENTAL METHODS

Simulation

As mentioned in the introduction that, surface plasmon resonance (SPR) will occur when the propagation constant of the incident light and propagation constant of SPPs (β_{SPPs}) match, and this is as defined by Equation (1) [18]:

$$\frac{2\pi n}{\lambda} \sin \theta = \beta_{SPPs}(\lambda, n_a). \quad (1)$$

Therefore, we can see the resonance phenomenon by observing the reflectance of the incident light. Figure 1 shows that the minimum reflectance resonance occurs at a certain angle (resonance angle θ_{res}). When the analyte's refractive index changes from the previous n_a to n_a^* , the resonance angle shifts from the previous one θ_{res} to θ_{res}^* . This phenomenon can be used to measure glucose and ethanol concentration in water because it affects the aqueous solutions' refractive index [19, 20].

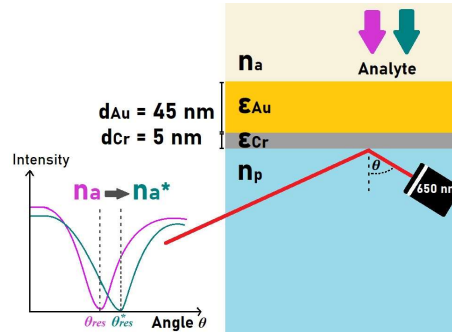


FIGURE 1. The scheme of the SPR sensor mechanism and the design in the simulation.

Figure 1 shows that the designed SPR sensor comprises Glass Prism/Cr/Au/Analyte layers in the structure, where the thickness of metallic layers is $d_{Cr} = 5$ nm of Cr (as an adhesion layer) and $d_{Au} = 45$ nm of Au. The refractive index of the glass prism was chosen as glass with $n = 1.52$, while the permittivity of Au (ϵ_{Au}) refers to Johnson and Christy (1972) [21] and Cr (ϵ_{Cr}) refers to Palik (1991) [22]. The light source was chosen, which is a monochromatic plane wave source that has a wavelength of 650 nm. To observe the reflectivity profile of the SPR sensor, we provided the reflection and transmission monitor. In the FDTD method, it is necessary to specify the boundary condition of the simulation region. We use a perfectly matched layer (PML) and Bloch boundary condition in this case. Moreover, to simulate the SPR sensor, we used the refractive index data of glucose-water mixtures, which follows the linear fit equations of refractive index-dependent glucose concentration by Belay and Assefa (2018) [19]. Meanwhile, to simulate ethanol concentration measurement in ethanol-water mixtures, we used the data from Vázquez-Guardado *et al.* (2019) [20]. The refractive index of glucose 3%, 5%, 8%, 10%, and 15% is 1.3337, 1.3370, 1.3420, 1.3453, and 1.3536 [19], whereas the refractive index of ethanol 7.21%, 24.2%, 41.51%, 71.23%, 83.55%, and 95.33% is 1.3372, 1.3493, 1.3572, 1.3631, 1.3631, 1.3608 [20].

Experiment

The SPR system with Kretschmann geometry used in the experiment consists of a prism coupled with a thin layer of gold, as shown in Fig. 2. In the measurement, a laser automatically shoots its beam toward the prism, forming the surface plasmon wave. As the laser light hit the thin gold layer, creating an evanescent wave. In the condition of internal reflection, surface plasmon and evanescent waves resonate, mutually reinforcing each other, generating the SPR phenomenon that was observed by changing the response unit to the angle variation displayed in the attenuated total reflection (ATR) graph.

We used two samples, i.e., ethanol and glucose solution, with varying concentrations in the measurement. The concentration of ethanol is 10%, 30%, 50%, 70%, and 100%, whereas the concentration of glucose is 0% (deionized water/ DI water), 6%, 8%, 10%, and 15%. Each sample was consecutively injected into the channel of the SPR system from the lower to higher concentration. DI water was used in the initial as a reference. The changes in the resonance angle were recorded.

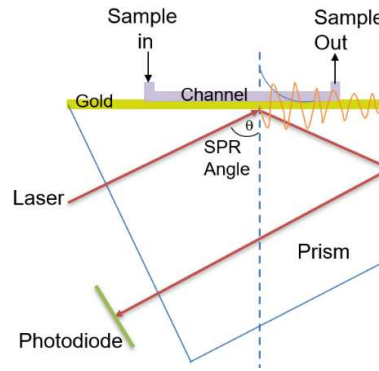


FIGURE 2. SPR system with Kretschmann configuration that was used in the experiment.

The SPR sensitivity (S) is referred to by the ratio between the shift of the wavelength or angle and the shift of the refractive index, as written in Equation (2) [23]:

$$S = \frac{\Delta\theta_{SPR}}{\Delta M} = \frac{\Delta\theta_{SPR}}{\Delta n} \frac{\Delta n}{\Delta M} \quad (2)$$

where $\Delta\theta_{SPR}$ is Resonance angle change, ΔM is sample concentration, and Δn is refractive index change. Since $\Delta n/\Delta M$ is constant, the sensitivity can be calculated by Equation (3):

$$S = \frac{\Delta\theta_{SPR}}{\Delta n} \quad (3)$$

RESULTS AND DISCUSSION

Figure 3(a) shows the simulation result of the SPR sensor of the glucose concentration measurement in water (aqueous solution) using the FDTD method. The sensor response in the simulation results shows a shift in the resonance angle if the concentration of solute changes. At concentrations 3%, 5%, 8%, 10%, and 15%, the resonance angles are located at 73.2881°, 73.7627°, 74.2373°, 75.6610°, and 76.1356°, respectively. Figure 3(b) describes the resonance angle trend corresponding to the glucose concentration variation. An increase in glucose concentrations causes an increase in its refractive indices. The coefficient of determination of the linear fitting is $R^2 = 0.9176$, which clarifies that the SPR sensor has good linearity for glucose concentration measurement in an aqueous solution. In this work, the sensor's sensitivity, as represented by Equation (3), is the slope of the linear trendline. Then, plotting between the resonance angles and refractive indices in [19] results in a linear trendline equation $y = 152.25x - 129.76$. Therefore, the sensitivity of glucose measurement has a value of $S = 152.25$ °/RIU.

A similar result occurred for the ethanol concentration measurement, as shown in Fig. 4(a), where a change in concentration causes a shift in the resonance angle. However, the trend is not linear in the higher concentration, as shown by the measurement at 71.23% and 83.55%. Their normalized reflected power curves are indistinguishable. Moreover, the resonance angle decreased when measurements were conducted at 83.55% and 95.33%. It can be seen that the resonance angle decreases from 78.03° to 77.56°, respectively. The trend of the simulated SPR sensor response for ethanol concentration is shown in Fig. 4(b). It can be seen that when at high concentrations, the resonance angle curve starts to decrease.

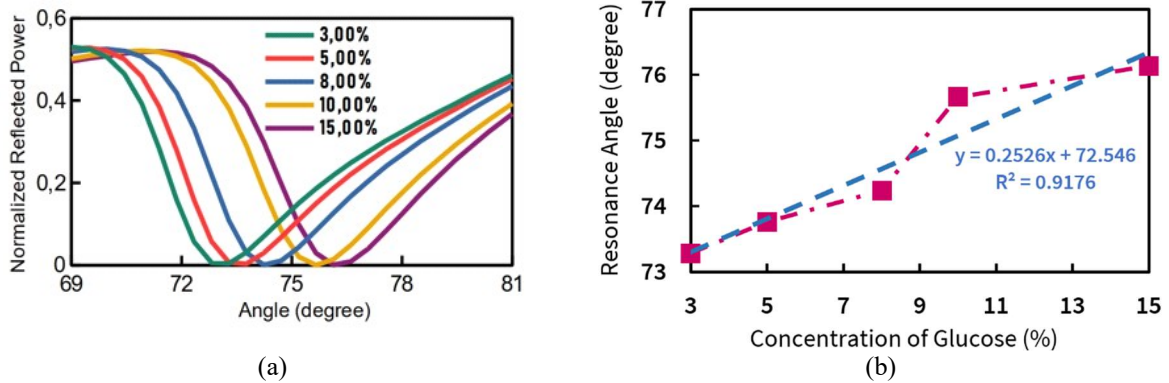


FIGURE 3. (a) Response curves of the simulated SPR sensor corresponding to variations in glucose concentration and (b) resonance angle as a function of glucose concentration.

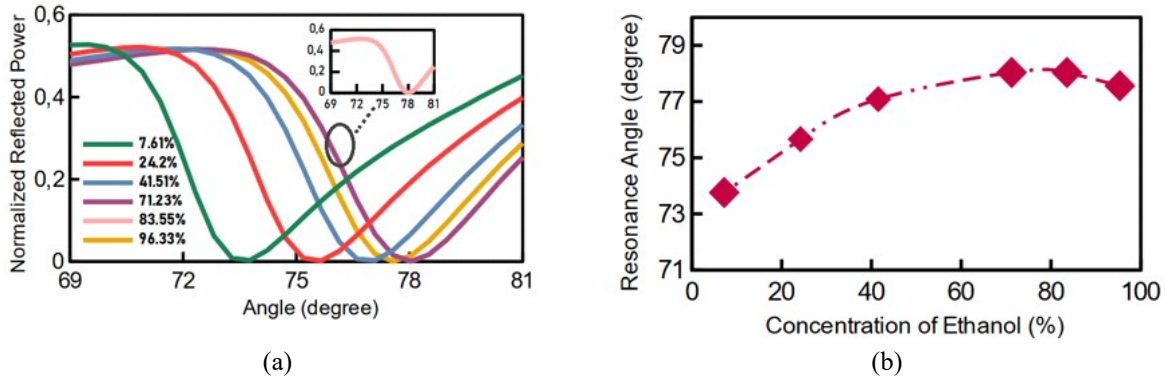


FIGURE 4. (a) Response curves of the simulated SPR sensor corresponding to variations in ethanol concentration and (b) resonance angle as a function of ethanol concentration.

Figure 5(a) shows the experimental result for the glucose measurement. The resonance angle for glucose with concentrations of 0%, 6%, 8%, 10%, and 15% is 71.607°, 73.108°, 73.503°, 73.838°, and 74.434°, respectively. It shows that the higher glucose concentration generates a higher resonance angle. Figure 5(b) shows that the resonance angle shifts higher as the glucose concentration increases, resulting in a linear trendline $y = 0.01899x + 71.817$ with $R^2 = 0.9639$. The change in resonance angle linearly corresponds to the refractive index change, and this relationship is proportional to the attached mass on the gold surface [24]. Moreover, to calculate the sensitivity for glucose measurement, we extracted refractive index (RI) data for glucose from [19], which has equation $y = 0.0017x + 1.328$. The refractive index for glucose was calculated using the equation, and the results show that the RI for glucose concentration of 0%, 6%, 8%, 10%, and 15% is 1.3280, 1.3382, 1.3416, 1.3450, and 1.3535, respectively. Therefore, the calculated sensitivity value (the slope of resonance angle as a function of the refractive index) is $S = 111.71^\circ/\text{RIU}$.

Figure 6(a) shows the response curves of the experimental SPR sensor corresponding to variations in ethanol concentration. The resonance angle for ethanol with concentrations of 10%, 30%, 50%, and 70% is 73.389°, 73.925°, 74.359°, and 74.359°, respectively. The difference in resonance angle is due to the different refractive indices of ethanol. These results agree with the previous experiment, where the resonance angle for the ethanol sample (100%) is higher than that for pure water [25]. From Figure 6(b), the resonance angle increases at a concentration of 10%,

30%, and 50%. However, the resonance angle is almost the same at 50% and 70% ethanol concentrations. This result agrees with the simulation result, where the resonance angle for the ethanol concentration is not always increasing. The conformity for a trend of detection between simulation and experiment of glucose and ethanol shows that the SPR sensor has good sensitivity and accuracy in detecting a small amount of glucose or ethanol so that in the future, this sensor can be used as a prospective sensor to detect chemical or biological compounds that have different refractive indices.

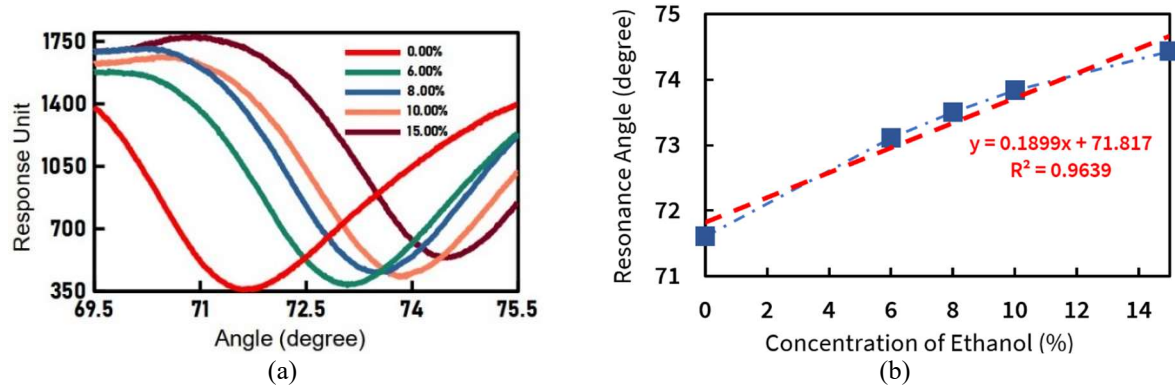


FIGURE 5. (a) Response curves of the experimental SPR sensor corresponding to variations in glucose concentration and (b) resonance angle as a function of glucose concentration.

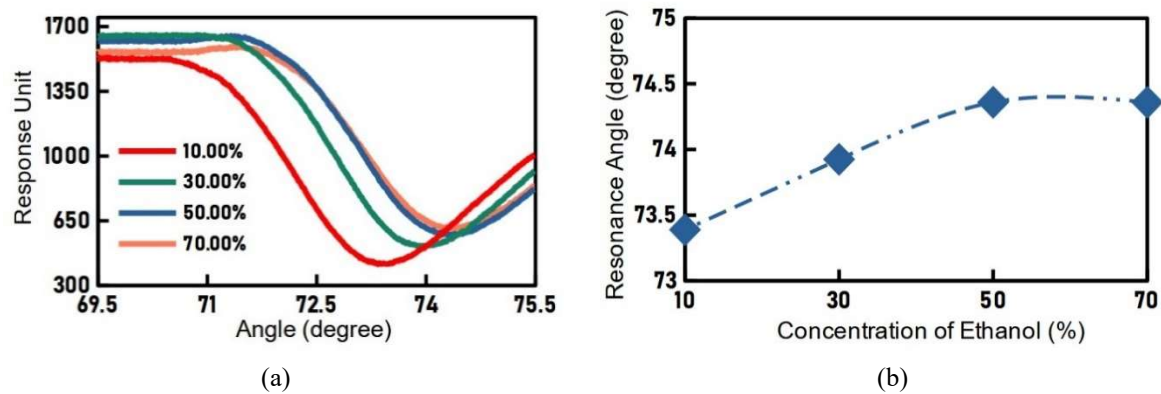


FIGURE 6. (a) Response curves of the experimental SPR sensor corresponding to variations in ethanol concentration and (b) resonance angle as a function of ethanol concentration.

CONCLUSION

The concentration of glucose and ethanol has been measured by an SPR sensor with Kretschmann configuration and studied by simulation and experiment through a resonance angle shift (SPR angle). The resonance angle shift corresponding to the solute concentration (glucose and ethanol) was monitored. From the simulation results, the resonance angle linearly increases of 73.2881° , 73.7627° , 74.2373° , 75.6610° , and 76.1356° as glucose concentrations increase from 3%, 5%, 8%, 10%, to 15%, respectively. The sensitivity of glucose detection was calculated to be $152.25^\circ/\text{RIU}$. From the simulation result, the resonance angle increases (71.607° , 73.108° , 73.503° , 73.838° , and 74.434° , respectively) as the concentration (0%, 6%, 8%, 10%, and 15%) increases, with the sensitivity of about $111.71^\circ/\text{RIU}$. The change in resonance angle linearly corresponds to the refractive index change. A similar result occurred for the ethanol concentration measurement, where an increase in concentration causes the resonance angle increases. However, the trend is not linear in the higher concentration. Meanwhile, in the simulation and experimental study of the ethanol measurement, the results conclude that the resonance angle is not constantly increasing as the concentration increases. All the experimental results agree with the simulation result, which indicated that SPR can possess prospective applications as a chemical sensor or medical diagnosis.

REFERENCES

1. J. Zhang, L. Zhang, and W. Xu, *J. Phys. D: Appl. Phys.* **45**, 113001 (2012).
2. Navratilova, and D. G. Myszka, "Investigating biomolecular interactions and binding properties using SPR biosensors," In *Surface plasmon resonance based sensors* edited by J. Homola (Springer, Berlin, 2006), pp. 155-176.
3. S. A. Maier, *Plasmonics: fundamentals and applications*, (Springer, New York, 2007), pp. 5–188. DOI: 10.1007/0-387-37825-1_2.
4. H. Yu, Y. Peng, Y. Yang, and Z. Li, *Npj Comput. Mater.* **5**, 1–14 (2019).
5. G. Baffou and R. Quidant, *Chem. Soc. Rev.* **43**, 3898–3907 (2014).
6. N. G. Khlebtsov, and L. A. Dykman, *J. of Quant. Spect. and Rad. Transfer* **111**, 1–35 (2010).
7. S. Balbinot, A. M. Srivastav, J. Vidic, I. Abdulhalim, and M. Manzano, *Trends in Food Sci. & Tech.* **111**, 128-140 (2021).
8. D. Wang, S. C. Pillai, S. H. Ho, J. Zeng, Y. Li, and D. D. Dionysiou, *Appl. Cat. B: Env.* **237**, 721-741 (2018).
9. R. B. Schasfoort, "History and Physics of Surface Plasmon Resonance," In *Handbook of Surface Plasmon Resonance* edited by R. B. Schasfoort (London, Royal Society of Chemistry, 2017), pp. 31 – 51.
10. Y. Zhao, Z. Q. Deng, and H. F. Hu, *IEEE Trans. on Instr. and Measurement* **64**, 3099-3104 (2015).
11. H. Saada, Q. Pagneux, J. Wei, L. Live, A. Roussel, A. Dogliani, L. D. Morini, I. Engelmann, E. K. Alidjinou, A. S. Rolland, E. Faure, J. Poissy, J. Labreuche, G. Lee, P. Li, G. Curran, A. Jawhari, J. A. Yunda, S. Melinte, A. Legay, J.L. Gala, D. Devos, R. Boukherroub, and S. Szunerits, *Sensors & Diagnostics* **1**, 1021-1031 (2022).
12. R. Nuryadi and R.D. Mayasari, *Applied Physics A* **122**, 1 – 6 (2016).
13. C. He, L. Liu, S. Korposh, R. Correia, and S. P. Morgan, *Sensors* **21**, 1420 (2021).
14. B. A. Prabowo, V. Purwidyantri, and K. C. Liu, *Biosensors* **8**, 80 (2018).
15. Y.-L. Yeh, *Opt. Lasers Eng.* **46**, 666-670 (2008).
16. H. Sobral and M. Pena-Gomar, *Appl. Opt.* **54**, 8453–8458 (2015).
17. C. M. Feng, Y. C. Huang, J. G. Chang, M. Chang, and C. Chou, *Opt. Commun.* **141**, 314–321 (1997).
18. S. Bellucci, V. Fitio, A. Bendziak, I. Yaremchuk, and Y. Bobitski, *Materials* **13**, 2989 (2020).
19. A. Belay and G. Assefa, *J. Lasers Opt. Photonics* **5**, 1000187 (2018).
20. A. Vázquez-Guardado, J. A. Ramirez-Flores, G. Lopez-Galmiche, J. J. Escobedo-Alatorre, and J. J. Sánchez-Mondragón, *Computación y Sistemas* **23**, 27-31 (2019).
21. P. B. Johnson and R. W. Christy, *Phys. Rev. B* **6**, 4370 (1972).
22. E. D. Palik, *Handbook of optical constants of solids*, (Academic press, New York, 1991), pp. 374-385.
23. L. Wu, H. S. Chu, W. S. Koh, and E. P. Li., *Opt. Express* **18**, 15458–15463 (2010).
24. T. Rudd, M. A. Skidmore, and E. A. Yates, "Surface-Based Studies of Heparin/Heparan Sulfate-Protein Interactions: Considerations for Surface Immobilisation of HS/Heparin Saccharides and Monitoring Their Interactions with Binding Proteins," In *Chemistry and Biology of Heparin and Heparan Sulfate* edited by H. G. Garg, R. J. Linhardt, and C. A. Hales, (Elsevier Science, Amsterdam, 2005), pp. 345-366. <https://doi.org/10.1016/B978-008044859-6/50013-7>.
25. N. Yanza, R. D. Mayasari, Y. Pradana, A. E. Mulyono, A. S. Budi, and R. Nuryadi, "A change of surface plasmon resonance (SPR) characteristics due to fluids type variation as a basic study of biosensor" In *The 8th National Physics Seminar-2019, AIP Conference Proceedings 2169*, edited by F. Bakri et al. (AIP Publishing, New York, 2019), pp. 060007. <https://doi.org/10.1063/1.5132685>.